Electronic Supplementary Information

Efficient Conversion of CO_2 and H_2O into Hydrocarbon Fuel over $ZnAl_2O_4$-Modified Mesoporous ZnGaNO under Visible Light Irradiation†

Shicheng Yan,[a,b]* He Yu,[a,c] Nanyan Wang,[a,c] Zhaosheng Li[a,b] and Zhigang Zou*[a,b,c]

[a] Eco-Materials and Renewable Energy Research Center (ERERC),National Laboratory of Solid State Microstructures, Nanjing University, Nanjing 210093, P. R. China. Fax: 86-25-83686632 ; Tel: 86-25-83686630
[b] College of Engineering and Applied Sciences, Nanjing University, Nanjing 210093, P. R. China.
[c] Department of physics, Nanjing University, Nanjing 210093, P. R. China.

Corresponding author E-mail: yscfei@nju.edu.cn (S.C.Yan); zgzou@nju.edu.cn (Z.G. Zou)

Experimental Section

Material preparation. A starting reagent, $NaGaO_2$ powder, was synthesized by heating a stoichiometric mixture of Na_2CO_3 and Ga_2O_3 at 850 ^oC for 12 h. The mixture of as-prepared $NaGaO_2$ and commercial $NaAlO_2$ (China National Medicines Corp. Ltd.) was dispersed in de-ionized water to form a colloidal suspension, magnetically stirred for 2h, and then, dried at 80 ^oC for 5h to get a gel. The gel was heated at 900 ^oC for 12 h for obtaining the $NaGa_{1-x}Al_xO_2$ solid solution.

To synthesize the mesoporous $Zn(Ga_{1-x}Al_x)_2O_4$, the $NaGa_{1-x}Al_xO_2$ colloidal suspension (0.2 M, 10 mL) was added into an aquatic solution of $Zn(CH_3COO)_2$ (0.05 M, 20 mL), stirred for 2 h at room temperature. The above-mentioned mixture was further heated in a 40 mL of Teflon-lined hydrothermal autoclave at 200 °C for 5 h for improving the crystallinity of $Zn(Ga_{1-x}Al_x)_2O_4$. The production was washed with de-ionized water, centrifuged and dried at 60 ^oC for 2 h, followed by nitriding it into $ZnAl_2O_4$-modified ZnGaNO solid solutions using a tubular furnace with an inner diameter of 50 mm at 700 ^oC for 5 h with an NH_3 flowing rate of 250 $mLmin^{-1}$. In addition, the mesoporous $ZnGa_2O_4$ was synthesized by ion exchange of $NaGaO_2$ and $Zn(CH_3COO)_2$ using the similar procedure to $Zn(Ga_{1-x}Al_x)_2O_4$, and then nitriding it into ZnGaNO solid solution using the similar route to $ZnAl_2O_4$-modified ZnGaNO.

Sample characterization. Crystal phases of these samples were determined using an X-ray diffractometer (XRD, Rigaku Ultima Ⅲ, Japan) operated at 40 kV and 40 mA using Cu Ka radiation. The diffuse reflectance spectra were recorded using a UV-Vis spectrophotometer (UV-2500, Shimadzu Co., Japan) and transformed to the absorption spectra according to the Kubelka-Munk relationship. The morphology was observed by using a transmission electron microscope (TEM, FEI Tecnai G2 F30 S-Twin, USA). Nitrogen absorption-adsorption isotherms were measured at 77 K on a Micromeritics ASAP 2000 volumetric adsorption analyzer. Before the measurements, the samples were pretreated at 200 ^oC for 2 h under flowing N_2 gas for clearing the surface. The BET specific surface areas were calculated using adsorption data acquired at a relative pressure (P/P_0) range of 0.05-0.15. The pore size distribution curves were calculated from the analysis of the adsorption branch of the isotherm using the Barrett-Joyner-Halenda (BJH) algorithm. The X-ray photoelectron spectroscopy (XPS) was obtained on PHI5000 Versa Probe (ULVAC-PHI, Japan) with monochromatized Al Kα x-ray radiation (1486.6 eV). The energy resolution of the electrons analyzed by the hemi-spherical mirror analyzer is about 0.2 eV. The binding energy was determined by reference to the C 1s line at 284.8 eV.

Photoreduction of CO_2. Pt cocatalyst was loaded on the catalyst surface by illuminating an aqueous CH_3OH solution (the volume ratio of CH_3OH to H_2O is 0.2) of $H_2PtCl_6{\cdot}6H_2O$ for about 10 h. The weight ratio of Pt to catalyst was 0.5 wt. %. In the photocatalytic reduction of CO_2, $ZnAl_2O_4$-modified ZnGaNO powder (0.1 g) was uniformly dispersed on a glass reactor with an area of 4.2 cm^2. The light irradiation system contains a 300 W Xe-lamp with cut-off filter L42 to achieve visible light ($\lambda \geq 420$ nm).The volume of the reaction system was about 230 mL. The reaction setup was vacuum-treated several times, and then, high purity CO_2 gas was introduced into the reaction to achieve ambient pressure. De-ionized water (0.4 mL) was injected into the reaction system as the

reducing agent. During irradiation, about 1 mL of gas was taken from the reaction cell at given intervals for subsequent CH_4 concentration analysis using a gas chromatograph (GC-2014; Shimadzu Corp., Japan).

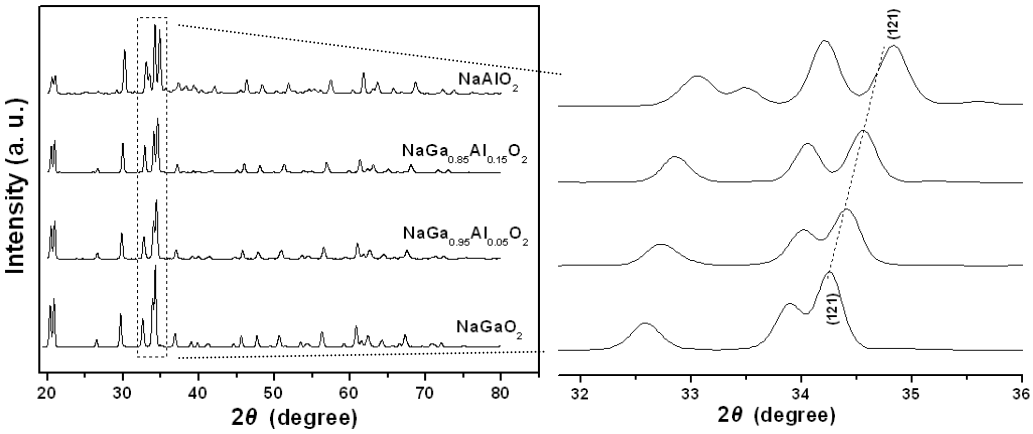

Fig. S1 XRD patterns for $NaGaO_2$ powder (JCPDS No 76-2151), $NaGa_{1-x}Al_xO_2$ (x=0.05, 0.15), and $NaAlO_2$ (JCPDS No 33-1200). Inset shows the diffraction peak position change of the (121) plane of the $NaGa_{1-x}Al_xO_2$. The peak position gradually shifted into the higher 2θ value with an increase in x value from 0 to 1 because the ion radius of Al^{3+} (0.57Å) is smaller than that of Ga^{3+} (0.62Å), indicating that the $NaGa_{1-x}Al_xO_2$ solid solution formed by calcining the mixed gel of $NaGaO_2$ and $NaAlO_2$.

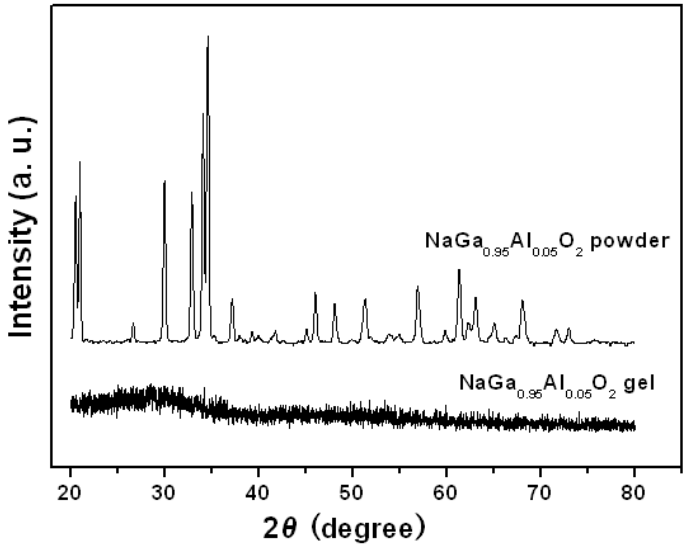

Fig. S2 XRD patterns for $NaGa_{0.95}Al_{0.05}O_2$ powder and gel.

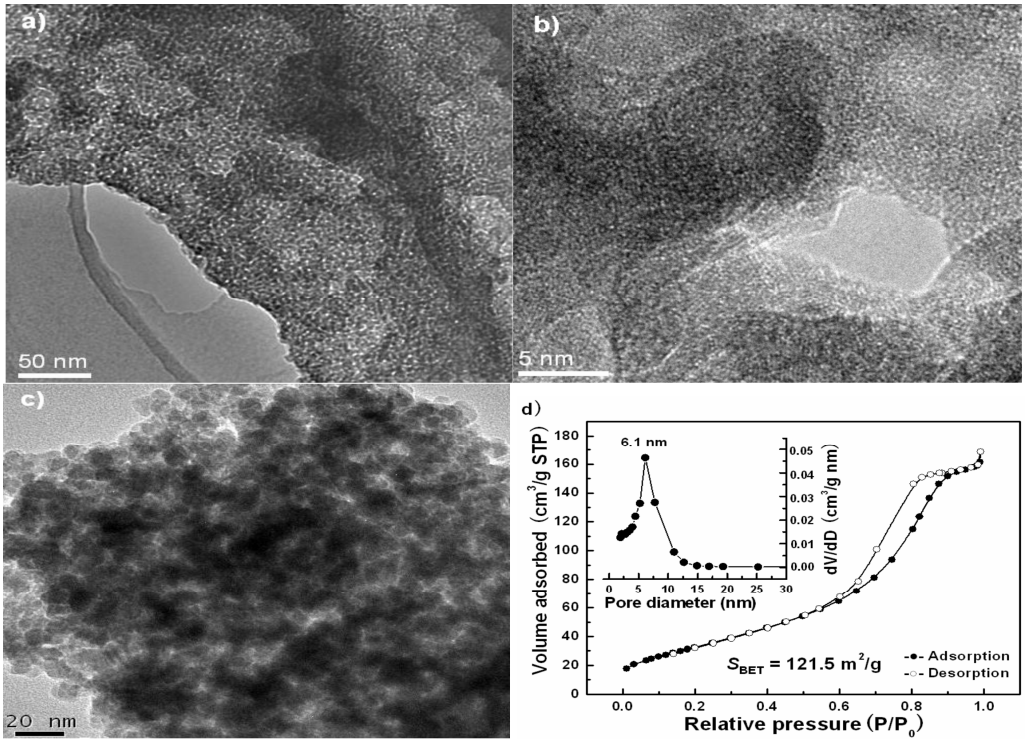

Fig.S3. a) TEM image for $NaGa_{1-x}Al_xO_2$ (x=0.05) colloidal particles. b) High-magnification TEM image of a typical mesopore in the $NaGa_{1-x}Al_xO_2$ (x=0.05) colloidal particles. c) TEM image of $Zn(Ga_{1-x}Al_x)_2O_4$ (x=0.05). d) Nitrogen absorption-desorption isotherms and pore-size distribution (inset) for $Zn(Ga_{1-x}Al_x)_2O_4$ (x=0.05).

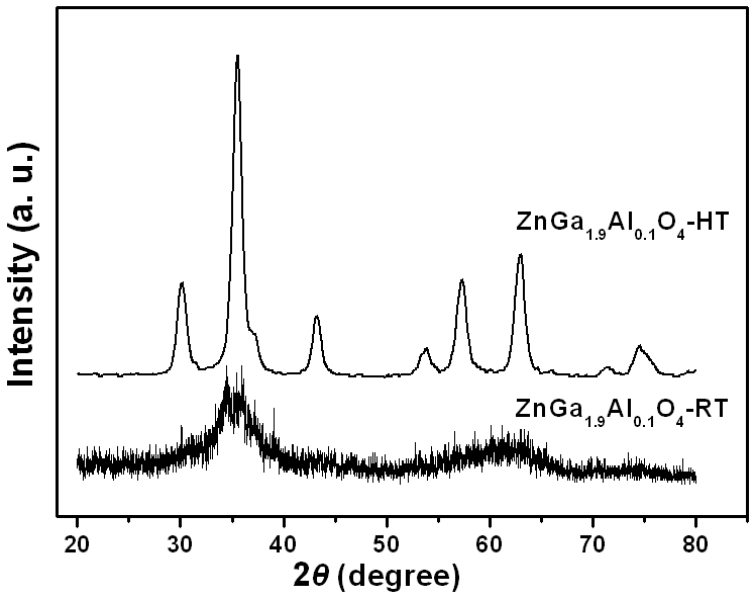

Fig. S4 XRD patterns for $ZnGa_{1.9}Al_{0.1}O_4$ obtained by room-temperature ion exchange (denoted as $ZnGa_{1.9}Al_{0.1}O_4$-RT) and hydrothermal treatment of $ZnGa_{1.9}Al_{0.1}O_4$-RT (denoted as $ZnGa_{1.9}Al_{0.1}O_4$-HT).

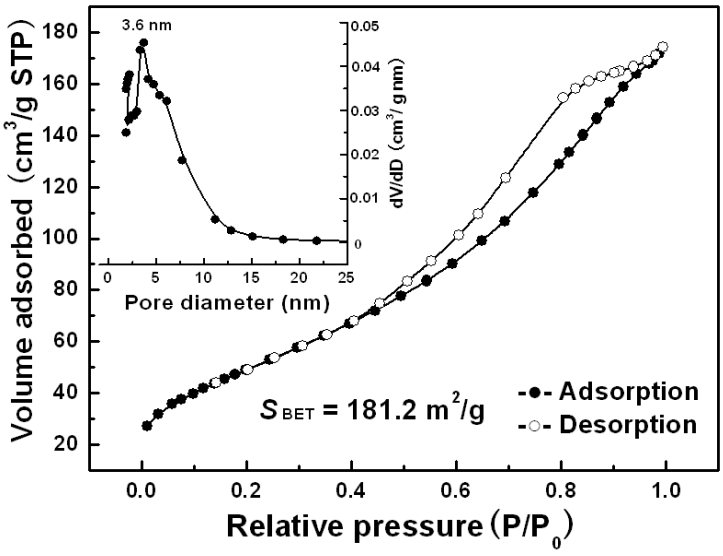

Fig. S5 Nitrogen absorption-desorption isotherms and pore-size distribution (inset) for $ZnGa_{1.9}Al_{0.1}O_4$ obtained by room-temperature ion exchange.

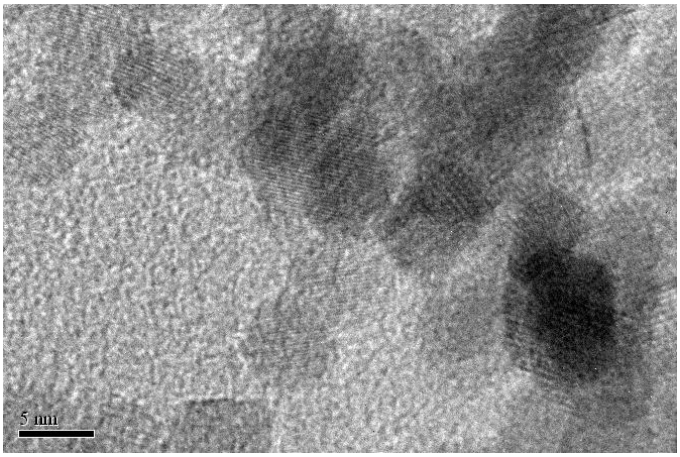

Fig. S6 HR-TEM image of $ZnGa_{1.9}Al_{0.1}O_4$ obtained by hydrothermal treatment

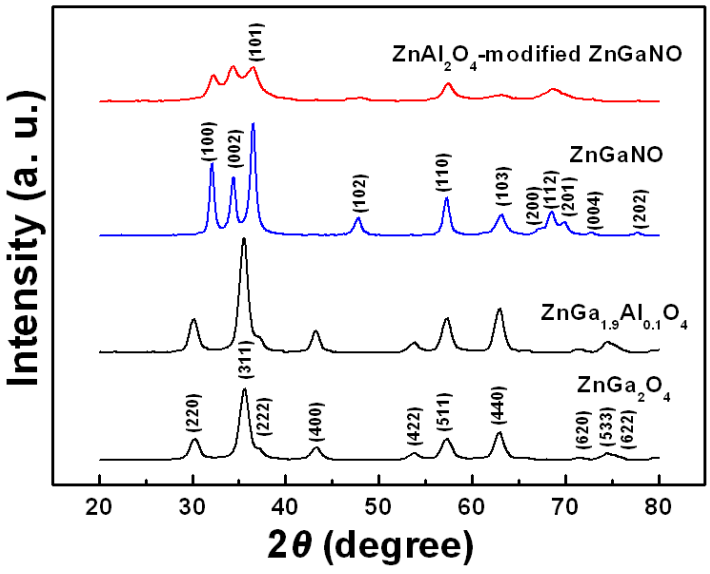

Fig.S7. XRD patterns for $ZnGa_2O_4$ (obtained by hydrothermal treatment of the product from room-temperature ion exchange of $NaGaO_2$ and $Zn(CH_3COO)_2$), $ZnGa_{1.9}Al_{0.1}O_4$ (obtained by hydrothermal treatment of the product from room-temperature ion exchange of $NaGa_{0.95}Al_{0.05}O_2$ and $Zn(CH_3COO)_2$), and their corresponding nitriding products: ZnGaNO and $ZnAl_2O_4$-modified ZnGaNO.

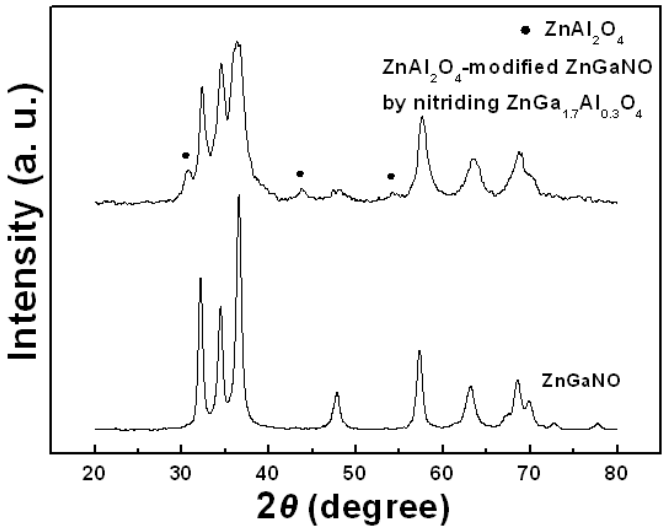

Fig. S8 XRD patterns for the $ZnAl_2O_4$-modified ZnGaNO (obtained by nitriding the $ZnGa_{1.7}Al_{0.3}O_4$) and ZnGaNO (obtained by nitriding the $ZnGa_2O_4$).

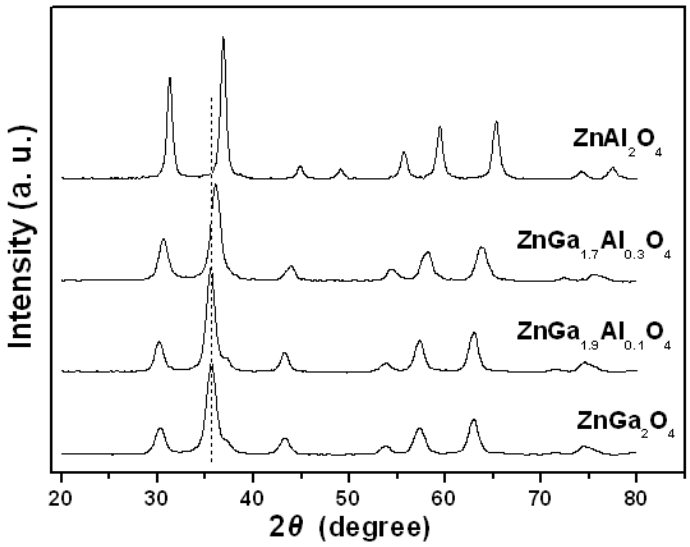

Fig. S9 XRD patterns for the $ZnGa_2O_4$, $ZnGa_{1-x}Al_xO_4$ (x=0.1, 0.3) and $ZnAl_2O_4$.

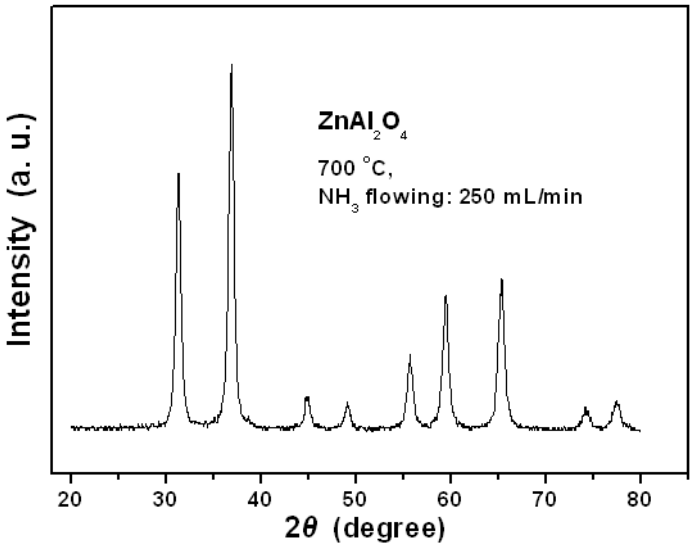

Fig. S10 XRD pattern for $ZnAl_2O_4$ obtained by heating a product from ion exchange of $NaAlO_2$ and Zn $(CH_3COO)_2$, at 700 ^oC under 250 mL min^{-1} of NH_3 flowing. The XRD pattern is in good agreement with JCPDS No 74-1136, indicating that the single-phase $ZnAl_2O_4$ formed.

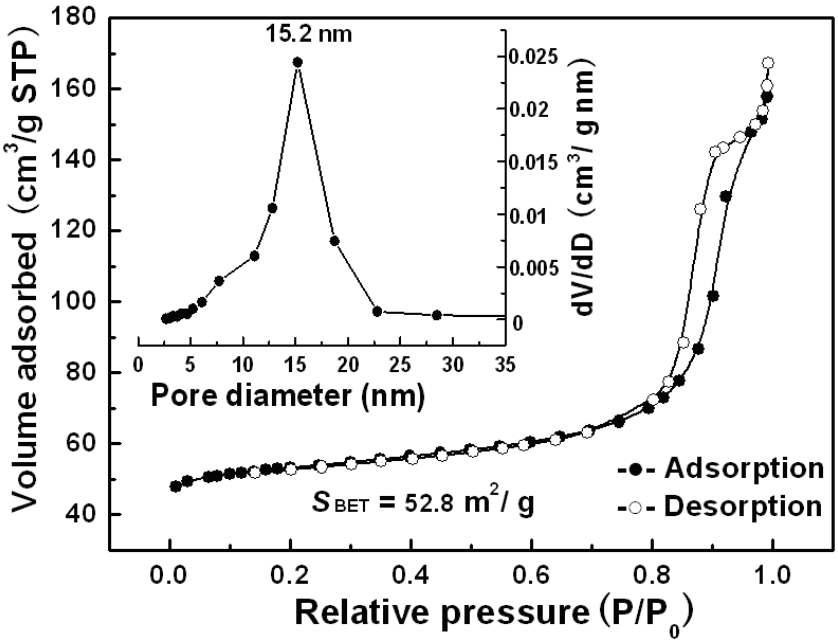

Fig.S11. Nitrogen absorption-desorption isotherms and pore-size distribution (inset) of $ZnAl_2O_4$-modified ZnGaNO

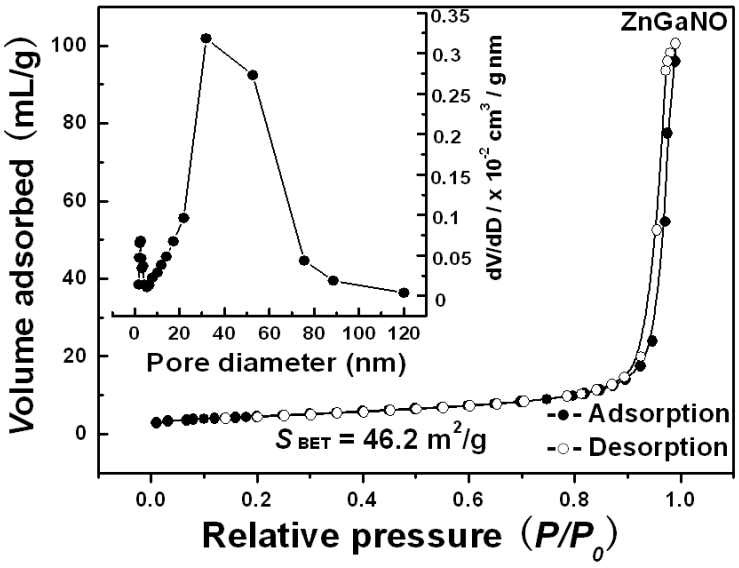

Fig. S12 Nitrogen absorption-desorption isotherms and pore-size distribution (inset) for ZnGaNO obtained by nitriding $ZnGa_2O_4$ at 700 ^oC.

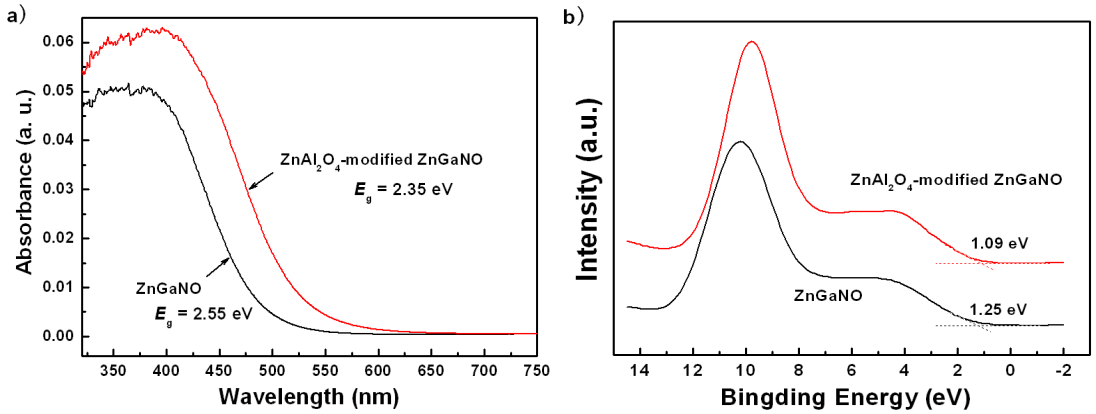

Fig.S13. a) UV-vis absorption spectra and b) VB XPS spectra for the ZnGaNO and $ZnAl_2O_4$-modified ZnGaNO. The band gap of $ZnAl_2O_4$ is about 4.5 eV.

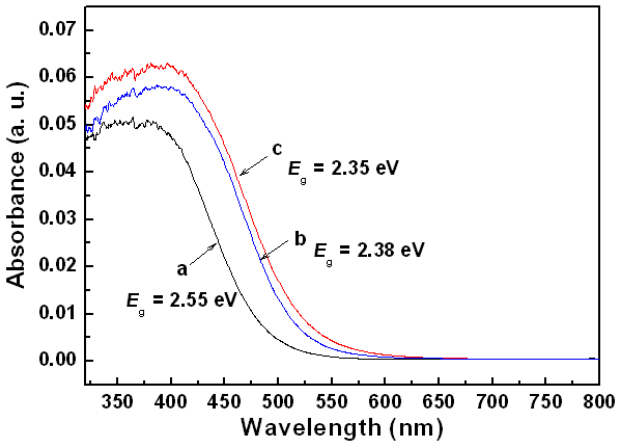

Fig. S14 UV-vis absorption spectra: ZnGaNO (curve a), $ZnAl_2O_4$-modified ZnGaNO obtained by nitriding $ZnGa_{1.7}Al_{0.3}O_4$ (curve b), and $ZnAl_2O_4$-modified ZnGaNO obtained by nitriding $ZnGa_{1.9}Al_{0.1}O_4$ (curve c).

Compared with the $ZnAl_2O_4$-modified ZnGaNO obtained by nitriding $ZnGa_{1.9}Al_{0.1}O_4$, the UV-Vis absorption spectrum of the $ZnAl_2O_4$-modified ZnGaNO obtained by nitriding $ZnGa_{1.7}Al_{0.3}O_4$ exhibited a blue shift of about 6 nm (Figure S15). This small shift probably resulted from the $ZnAl_2O_4$ content in the ZnGaNO obtained by nitriding $ZnGa_{1.7}Al_{0.3}O_4$ increases, which lead to the relative Zn content in ZnGaNO decreases. This also indicates that the high Al content in $Zn(Ga_{1-x}Al_x)_2O_4$ precursor is not beneficial for improving the Zn content in the ZnGaNO product.

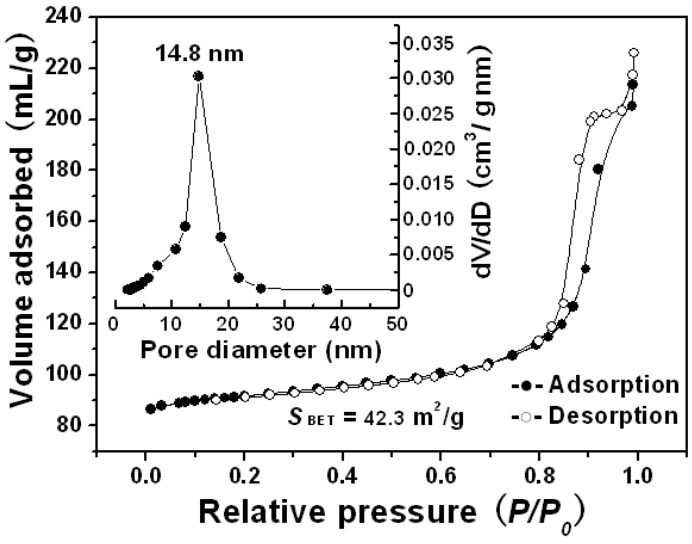

Fig. S15 Nitrogen absorption-desorption isotherms and pore-size distribution (inset) for $ZnAl_2O_4$-modified ZnGaNO obtained by nitriding $ZnGa_{1.7}Al_{0.3}O_4$.

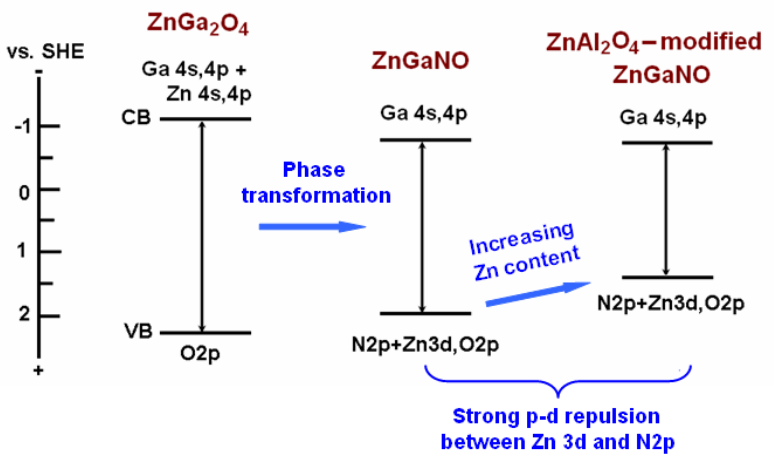

Fig. S16 Schematic band structures for the $ZnGa_2O_4$, ZnGaNO and $ZnAl_2O_4$-modified ZnGaNO

For the semiconducting $ZnGa_2O_4$ with a band gap of 4.4 eV, the valence band was mainly composed of the O2p orbitals and the conduction band was formed by hybridization of Ga 4s4p and Zn 4s4p orbitals. By nitriding treatment of $ZnGa_2O_4$, the ZnGaNO solid solution with a band gap of about 2.55eV can be obtained. The valence band edge of ZnGaNO primarily derives from Zn 3d, N 2p and O 2p orbitals and the conduction band edge from Ga 4s,4p orbitals. In particular, the presence of Zn3d and N2p electrons in the upper valence band provides p-d repulsion for the

valence band maximum, which results in narrowing the band gap. Therefore, increasing the Zn content in the ZnGaNO can increase the valence band by the strong p-d repulsion between Zn 3d and N 2p. $ZnAl_2O_4$-modified ZnGaNO was obtained by nitriding the $Zn(Ga_{1-x}Al_x)_2O_4$.The phase separation occurred during the nitriding, that is, the $ZnAl_2O_4$ in situ formed during the phase transformation from $ZnGa_2O_4$ to ZnGaNO. The formation of the $ZnAl_2O_4$ can prevent the Zn volatilization due to its chemical inertness. Therefore, the $ZnAl_2O_4$-modified ZnGaNO has high Zn content, thus having the small band gap.

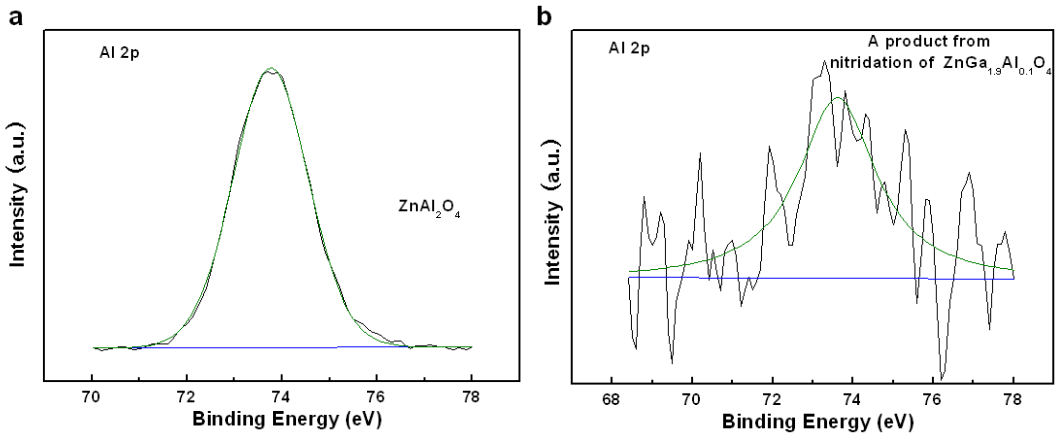

Fig. S17 Al2p XPS spectra: a) $ZnAl_2O_4$, b) $ZnAl_2O_4$-modified ZnGaNO (obtained by nitriding $ZnGa_{1.9}Al_{0.1}O_4$). The peak at 73.46 eV for Al2p of $ZnAl_2O_4$ is basically consistent with the Al2p of the product from nitriding of $ZnGa_{1.9}Al_{0.1}O_4$, indicating that the $ZnAl_2O_4$ occurred during the nitriding $ZnGa_{1.9}Al_{0.1}O_4$.

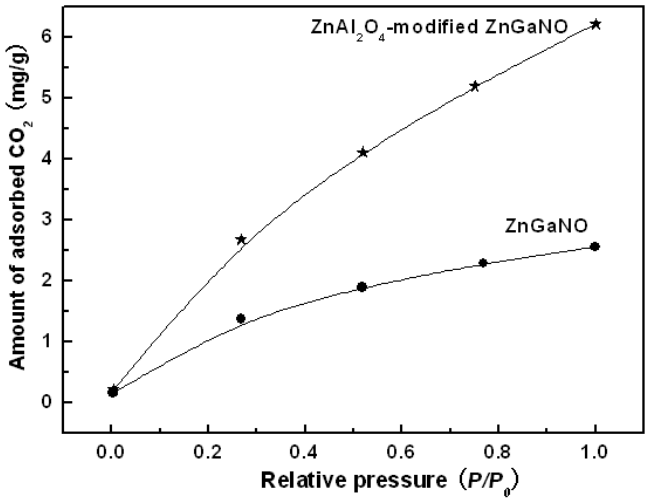

Fig. S18 CO_2 absorption isotherms for ZnGaNO and $ZnAl_2O_4$-modified ZnGaNO.

The amount of physisorbed CO_2 was determined by a BET method at 0 ^oC. The ZnGaNO and $ZnAl_2O_4$-modified ZnGaNO were pretreated at 200 ^oC for 2h under flowing N_2 gas for clearing the surface. The CO_2 adsorption was carried out on a surface area analyzer (Micrometrics Co., USA). The CO_2 was firstly adsorbed on the surface of powder samples at 0 ^oC by a standard adsorption procedure same to N_2 adsorption used in the specific surface area test (first adsorption).

After reaching the gas adsorption equilibrium, the powder sample was vacuum-treated. After that, the CO_2 adsorption was again carried out (second adsorption). In the second CO_2 adsorption test, the powder sample mainly exhibited a physisorption process because the chemisorbed CO_2 in the first adsorption test does not be removed by vacuum-treating, but the physisorbed CO_2 does. Therefore, the amount of physisorbed CO_2 was determined using the second adsorption test.

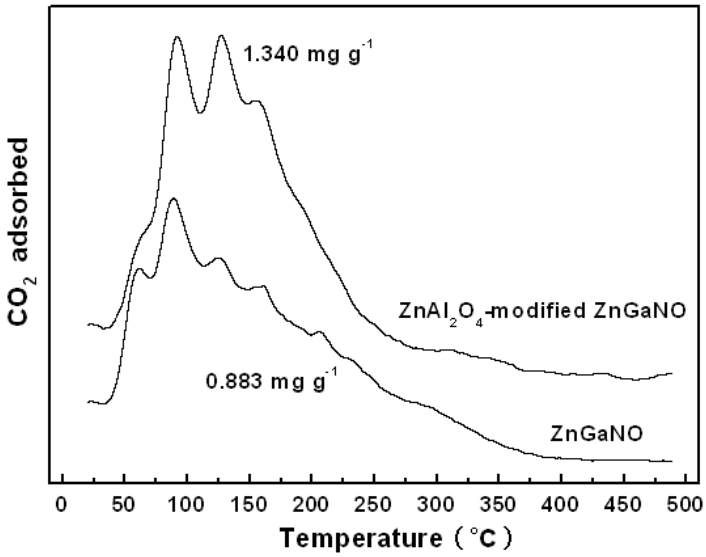

Fig. S19 CO_2-TPD profiles of ZnGaNO and $ZnAl_2O_4$-modified ZnGaNO.

In a typical CO_2-TPD experiment, the sample was activated at 500 ^oC for 2 h prior to the adsorption of CO_2 at 25 ^oC. After purging the physically adsorbed CO_2 at 25 ^oC, the sample was heated to 500 ^oC at a rate of 8 ^oC min^{-1}.

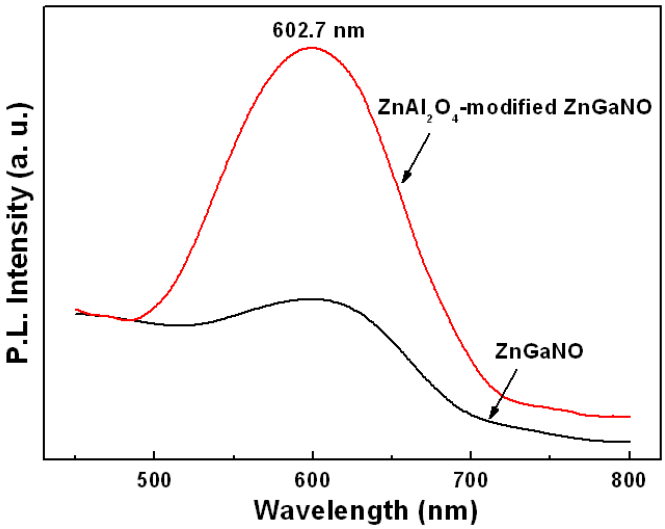

Fig. S20 Room temperature PL spectra for the as-prepared ZnGaNO and $ZnAl_2O_4$-modified ZnGaNO. Excitation at 380 nm.

In a previous study [M. Yashima, K. Maeda, K. Teramura, T. Takata, K. Domen, *Chem. Phys.Lett.* 2005, 416, 225], it was confirmed that the ZnGaNO solid solution exhibits photoluminescence (PL) resulting from the recombination of photogenerated electrons and holes.

The PL process is largely governed by the presence of surface vacancies and defects since they act as recombination centers for photogenerated electrons and holes. In our case, the photoluminescence (PL) spectroscopy was obtained by using the Cary eclipse fluorescence spectrophotometer. The ZnGaNO and $ZnAl_2O_4$-modified ZnGaNO exhibit a PL band at around 602 nm upon photoexcitation at 380 nm, as shown in Fig.S14. It can be seen that the intensity of the PL band of the $ZnAl_2O_4$-modified ZnGaNO is higher than that of the ZnGaNO, suggesting that the recombination centers of the electrons and holes were increased, probably due to the Zn^{2+} or Ga^{3+} defects from the $ZnAl_2O_4$ phase separation during the nitriding $ZnGa_{1.9}Al_{0.1}O_4$. For the $ZnAl_2O_4$-modified ZnGaNO, the $ZnAl_2O_4$ occurred during the nitridation of $ZnGa_{1.9}Al_{0.1}O_4$. This phase separation process may increase the formation of some defects such as Ga^{3+} and Zn^{2+} vacancies, which usually are Lewis base sites. CO_2 is adsorbed on the base site easily, and then the conformation of a linear CO_2 molecule undergoes a great change. The adsorption of CO_2 contributes to the photocatalytic reduction of CO_2.

The water adsorption on these as-prepared samples was also investigated by weighing method. These weighed as-prepared samples were spread on the surface of glass plate with about 4.2 cm^2, and put into a closed desiccator. The water adsorption was performed under 75% humidity at 35 ^oC for 24 h. These samples were weighed again after water adsorption. The amount of increase in weight is the amount of water adsorbed on the sample. The amount of water adsorbed on the $ZnAl_2O_4$-modified ZnGaNO was determined to be 0.212 g/g, which is about 4 times as high as the adsorbed amount of 0.056 g/g for the ZnGaNO, probably due to the mesoporous structure and improved surface area.

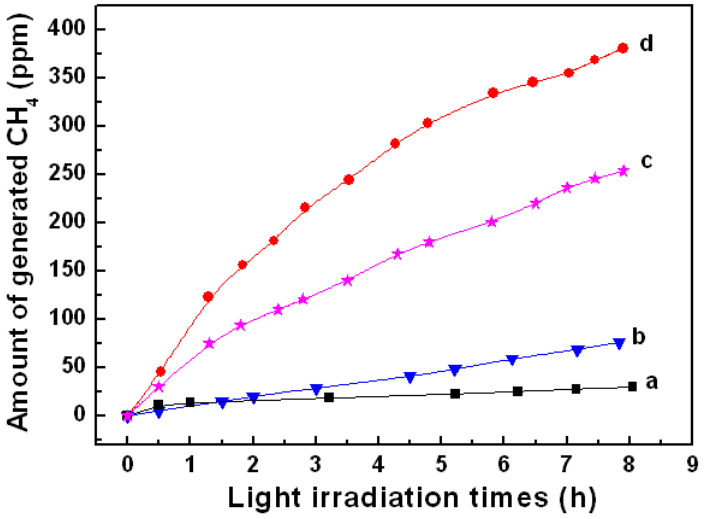

Fig. S21 CH_4 generation over N-doped TiO_2 (curve a), ZnGaNO (curve b), $ZnAl_2O_4$-modified ZnGaNO obtained by nitriding $ZnGa_{1.7}Al_{0.3}O_4$ (curve c), and $ZnAl_2O_4$-modified ZnGaNO obtained by nitriding $ZnGa_{1.9}Al_{0.1}O_4$ (curve d), as a function of irradiation time. The all catalysts were modified by loading 0.5 wt.% Pt as co-catalyst.

Compared with the $ZnAl_2O_4$-modified ZnGaNO obtained by nitriding $ZnGa_{1.9}Al_{0.1}O_4$, the photocatalytic activity in photoreduction CO_2 for $ZnAl_2O_4$-modified ZnGaNO obtained by nitriding $ZnGa_{1.7}Al_{0.3}O_4$ decreased (Figure S17). The $ZnAl_2O_4$-modified mesoporous ZnGaNO obtained by nitriding $ZnGa_{1.7}Al_{0.3}O_4$ exhibited a CH_4 generation rate of 49.7 ppm h^{-1} during the

first hour under visible light illumination. The specific surface area of the $ZnAl_2O_4$-modified ZnGaNO obtained by nitriding $ZnGa_{1.7}Al_{0.3}O_4$ (42.3 m^2/g) (Figure S16) is lightly lower than that of the $ZnAl_2O_4$-modified ZnGaNO obtained by nitriding $ZnGa_{1.9}Al_{0.1}O_4$ (52.8 m^2/g), however, the $ZnAl_2O_4$ content in the former is higher than that in the later. This means that the more $ZnAl_2O_4$ dispersed on the surface of the $ZnAl_2O_4$-modified ZnGaNO obtained by nitriding $ZnGa_{1.7}Al_{0.3}O_4$, which decreased the reaction sites, thus decreased photocatalytic activity.

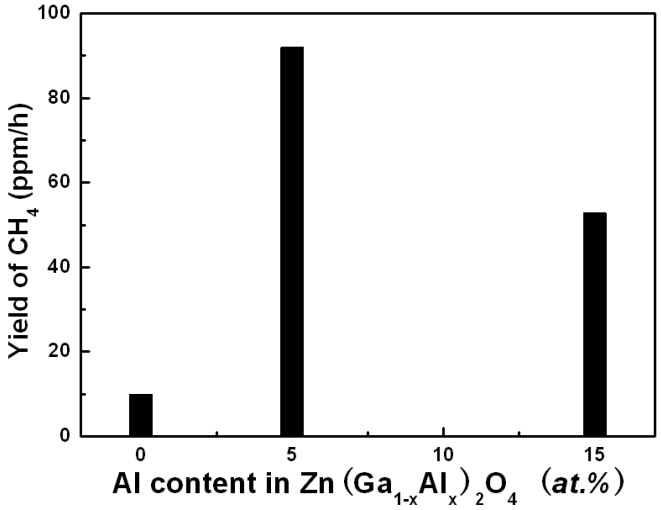

Fig. S22 CH_4 generation rate over the ZnGaNO (0 at. % Al), $ZnAl_2O_4$-modified ZnGaNO obtained by nitriding the $ZnGa_{1.9}Al_{0.1}O_4$ (5 at.% Al) and $ZnAl_2O_4$-modified ZnGaNO obtained by nitriding the $ZnGa_{1.7}Al_{0.3}O_4$ (15 at.% Al). The all catalysts were modified by loading 0.5 wt.% Pt as co-catalyst. Apparently, the $ZnAl_2O_4$-modified ZnGaNO obtained by nitriding the $ZnGa_{1.9}Al_{0.1}O_4$ exhibited the best photocatalytic activity.

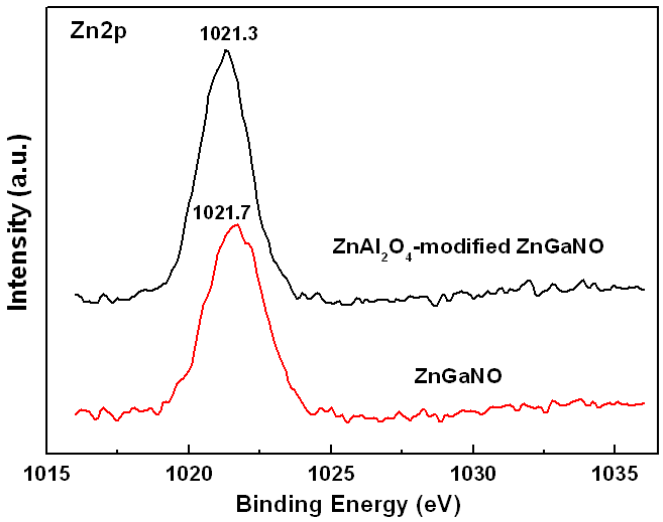

Fig. S23 Zn2p XPS spectra for ZnGaNO and $ZnAl_2O_4$-modified ZnGaNO.

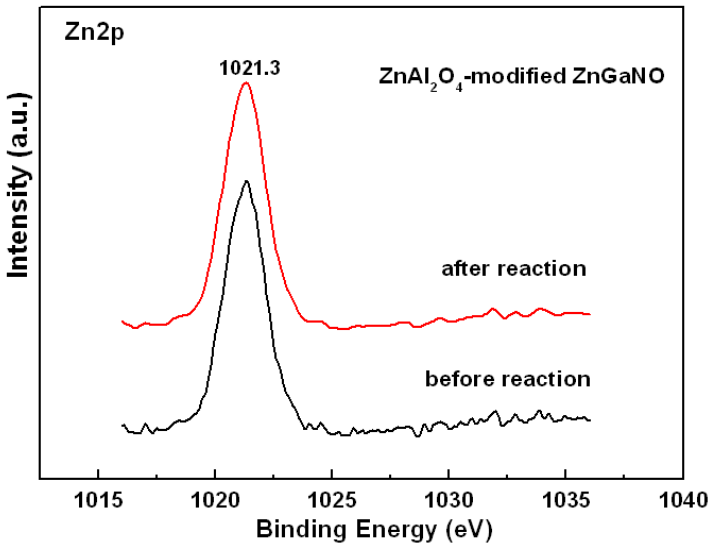

Fig. S24 Zn2p XPS spectra for $ZnAl_2O_4$-modified ZnGaNO before reaction and after reaction.

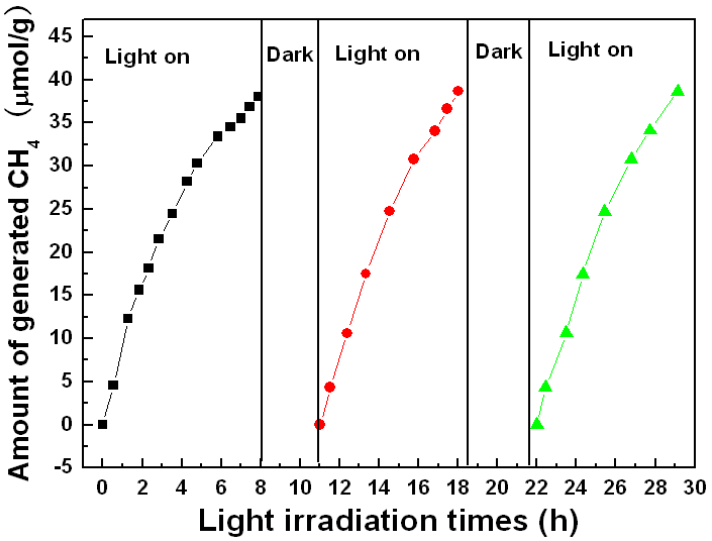

Fig. S25 CH_4 generation over $ZnAl_2O_4$-modified ZnGaNO in three reaction cycles as a function of irradiation time.

In the three reaction cycles, the CH_4 generation rate in second reaction cycle is 7.4 μmol $g^{-1}h^{-1}$, which is about 19% lower than that in the first reaction cycle. However, the CH_4 generation rate in third reaction cycle is similar to that in the second reaction cycle to be 7.2 μmol $g^{-1}h^{-1}$. This indicates that the photocatalytic performance of $ZnAl_2O_4$-modified ZnGaNO is stable.

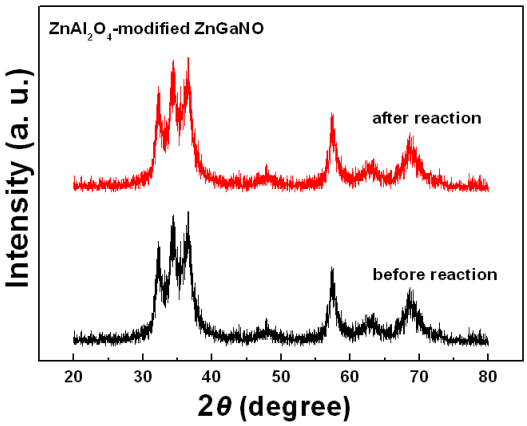

Fig. S26 XRD patterns for $ZnAl_2O_4$-modified ZnGaNO before reaction and after reaction.